Journal of Scientific & Industrial Research
Vol. 84, May 2025, pp. 509-519
DOI: 10.56042/jsir.v84i5.9965

Superhydrophobic Silica-based Nano-Coatings for Anti-Reflective and Anti-Soiling Surface: Effect of HMDS and DIPEA

Abhineet Samadhiya[1,3], Pradeep Kumar Jhinge[1] & Kamal Kumar Kushwah[2]*

[1]Department of Mechanical Engineering, [2]Department of Applied Physics, Jabalpur Engineering College, Jabalpur 482 011, India

[3]Rajiv Gandhi Proudyogiki Vishwavidyalaya, Bhopal 462 033, India

Received 27 March 2024; revised 14 November 2024; accepted 17 March 2025

This study presents a novel nano-silica-HMDS (hexamethyldisilazane) surface coating, synthesized through an efficient chemical route, exhibiting anti-reflective, superhydrophobic, and anti-soiling properties suitable for solar panel top covers working in dusty environments. The synthesized surface coating enhances optical transmission, mitigating incident light reflection and performance loss from soiling. The experiment results show a 5.8% average power improvement in the nano-silica-HMDS-coated solar photovoltaic cell compared to a manually cleaned, uncoated solar cell. The cost-effective dip-coating method applied to the substrate surface at room temperature offers a practical alternative to costly surface coatings. The surface coating exhibits a finely tuned refractive index of 1.14 and 96.1% transmittance for wavelengths ranging from 400–800 nm demonstrating exceptional transparency and optical effectiveness. The Field Emission Scanning Electron Microscopy (FESEM) and Atomic Force Microscopy (AFM) results show a highly rough HMDS-modified-nano-silica surface exhibiting anti-soiling and super-hydrophobicity characteristics confirmed by a water contact angle of 156° in test results. The synthesized surface coating also showed excellent stability over two months in a dusty environment consisting of abundant particulate particles pm 2.5 and pm 10 observed in environmental stability tests conducted over 2.5 months with the help of an experimental setup. The test results confirm the nano-silica-HMDS (0.3:1) surface coating as the most optimum concentration for simultaneously achieving superhydrophobicity, anti-soiling, and antireflection properties.

Keywords: Coating performance, Enhanced solar efficiency, Multifunctional nano-coatings, Solar cell optimization, Surface modification

Introduction

The effective harvesting of solar energy has driven an ongoing quest for advancements in photovoltaic technology. A major challenge hindering the efficiency and performance of solar panels is the accumulation of dust, dirt, and water droplets on their surfaces, which increases the reflection of incident light and reduces energy conversion. Consequently, minimizing the reflection of incident light and mitigating surface soiling is critical to improving the performance of solar photovoltaic panels.

Reflection primarily occurs at the air-glass interface, where the transparent substrate's reflective properties influence the overall efficiency of solar modules.[1–3] To address this, extensive research has been conducted on developing anti-reflective coatings with optimized Refractive Indices (RI) to minimize unwanted reflections.[4,5] According to the principles of optical interference and the Fresnel equation, the ideal refractive index for optical glass is approximately 1.5, while for air, it is around 1.0. This suggests that the optimal RI for a single-layer anti-reflective coating should fall within the range of 1.20 to 1.25.[(6)]

Achieving this appropriate refractive index requires careful control over the porosity of the coated surface to minimize optical losses at the substrate interface.[7] At the same time, maintaining high transparency of the substrate is essential, which typically demands regular physical cleaning. However, frequent cleaning can damage the anti-reflective coating, accelerating the loss of transmittance over time.[8,9] Moreover, basic anti-reflective coatings often fail to meet the performance requirements in polluted environments, particularly for applications such as solar photovoltaic panels, decorative glass, and automobile glass.[10,11]

Recent research addresses these challenges by exploring the integration of self-cleaning properties into anti-reflective coatings. Hydrophobicity, achieved through micro-structured or nano-structured surfaces combined with low-surface-energy materials, has been identified to be a key factor influencing self-cleaning

*Author for Correspondence
E-mail: kamal_kushwah2005@yahoo.com

performance.[12–14] As a result, the dual functionality of anti-reflective and anti-soiling properties has garnered considerable attention over the past few decades.

Initial studies predominantly focused on anti-reflective coatings to reduce reflection losses, utilizing dielectric materials as the primary solution.[15–17] While these efforts provided valuable insights, they largely overlooked the incorporation of hydrophobic features, which are crucial for addressing soiling issues in solar photovoltaic applications. As research progressed, the role of environmental conditions on solar cell performance became clearer, prompting increased interest in hydrophobic coatings to mitigate soiling effects.[18–21] In recent years, significant advancements have been made in developing various nanomaterial-based surface coatings that combine super-hydrophobic and anti-reflective properties suitable for various applications.[22–25]

Despite this noteworthy progress, limited attention has been given to surface coatings with combined properties for application in solar photovoltaic cells. Although some notable advances have been achieved in anti-reflective coatings and hydrophobic treatments, the innovative integration of superhydrophobic, anti-reflective, and anti-soiling properties into a single nano-coating to enhance solar cell efficiency and evaluate their environmental performance remains an unresolved research gap. A simplistic and comprehensive approach that seamlessly integrates these properties with proper experimental investigation and real-time environmental monitoring and evaluation remains absent from the scientific literature.

In this study, we investigated the stability and environmental response of synthesized nano-silica-based surface coatings incorporating HMDS and diisopropylethylamine. The nano-silica-HMDS (0.3:1) was observed as the most optimum surface coating based on superior water contact angle and transparency test results. It also exhibits exceptional stability when applied to the solar photovoltaic cell's surface confirmed by the experimental testing for over 2.5 months, successfully demonstrating superhydrophobicity, anti-soiling, and antireflection properties. Hence, it is suitable to be used as a surface coating for solar photovoltaic applications installed in dusty environments.

Material and Methods

Materials used

The research employed finely ground and powdered silicon dioxide nanoparticles with typical particle sizes of 35–40 nm and a binding silane agent, namely, hexamethyldisilazane (HMDS). Other reagents, such as di-isopropyl ethyl amine (DIPEA), distilled water, and anhydrous ethanol, were used in their original configuration without any previous or subsequent purification. The step-by-step synthesis procedure is depicted in Fig. 1. All substances were of the appropriate analytical grade. All materials and associated chemicals were purchased from Sigma-Aldrich Private Limited.

Preparation of the HMDS-Modified Nano-Silica Particles

Nano-silica and HMDS were synthesized with mass ratios of 0.3:1, 0.5:1, 1:1, 1:0.3, and 1:0.5. They were thoroughly suspended in 280 mL of anhydrous ethanol and ultrasonicated separately for 1 h at 80°C. The acquired products were then washed and filtered, and the solid portion was set up in a vacuum-dry oven at 55℃ for 24 h. Finally, nano-silica-HMDS was acquired.

The reaction of nano-silica (SiO_2) with hexamethyldisilazane ($(((CH_3)_3Si)2NH)$) in the presence of diisopropylethylamine ($((CH_3)2CH)2NC_2H_5$ involves following steps:

Surface Hydroxylation of Nano Silica

Nano silica (SiO_2) typically has surface hydroxyl groups (-OH) due to adsorbed water or intrinsic surface properties. This can be represented as:

SiO_2 (nano-silica) + H_2O → SiO_2-OH (silanol groups)

Reaction of Silanol Groups with Hexamethyldisilazane (HMDS)

Hexamethyldisilazane (HMDS) interacts with the nano-silica's surface hydroxyl groups. Ammonia (NH_3) is released as a byproduct of the process, which includes substituting a trimethylsilyl group ($-Si(CH_3)_3$) for the hydroxyl group. The reaction taking place can be systematically represented as

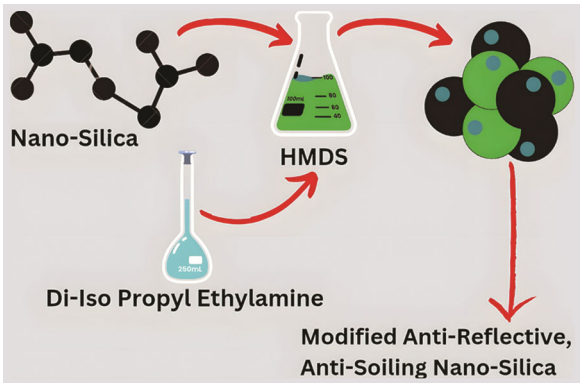

Fig. 1 — Schematic representation of the sequential preparation of modified anti-reflective and anti-soiling nano-silica-HMDS coatings

follows: SiO_2-OH → SiO_2-O-Si$(CH_3)_3$ + NH_3 + $((CH_3)_3Si)2NH$

Function of Diisopropylethylamine (DIPEA)

Di-isopropyl-ethylamine (DIPEA) specifically acts as a strong base, facilitating deprotonation of hydroxyl groups (Si-OH) on the nano-silica surface. This deprotonation generates a nucleophilic species that reacts efficiently with hexamethyldisilazane (HMDS), enabling the grafting of hydrophobic Trimethylsilyl (-Si$(CH_3)_3$) groups onto the silica surface. Without DIPEA, the reaction would proceed less efficiently, potentially leaving residual hydroxyl groups that reduce the hydrophobicity of the coating. The presence of DIPEA also stabilizes the intermediate species and prevents undesired side reactions, ensuring uniform surface modification.

Formation of Modified Silica Surface

Trimethylsilyl groups are deposited on the surface of the silica nanoparticles because of the following reaction:

SiO_2 (nano-silica) + $((CH_3)3Si)$ 2NH → SiO_2-O-Si$(CH_3)_3$ (trimethylsilyl silica) + NH_3

The overall reaction can be represented as follows:

SiO_2 + 2 $((CH_3)3Si)$ 2NH → SiO_2 $(O\text{-}Si(CH_3)_3)_2$ + 2 NH_3

In the above equation, SiO_2 $(O\text{-}Si(CH_3)_3)_2$ represents the nano-silica surface fully modified with trimethylsilyl groups.

Preparation of Dual-Functional Coatings

Glass slides 75 mm × 26 mm with 1 mm thickness without any pre-treatment procedures were used as a substrate for creating a dual-functioning coating cleaned using ethanol absolute as well as deionized water. The anti-reflection coating was prepared by depositing a modified nano-silica solution onto the glass substrate using dip-coating. The dip-coating method was chosen specifically because it is well-known for its cost-effectiveness due to its simple setup, minimal material waste, and scalability, making it a viable alternative to high-vacuum-based deposition techniques such as Physical Vapor Deposition (PVD) and Chemical Vapor Deposition (CVD), which require expensive equipment, controlled environments, and extensive energy consumption. Furthermore, unlike spray-coating, dip-coating offers better coating homogeneity and thickness control, decreasing material loss and assuring repeatability. The resulting coating is highly durable due to its strong adherence and consistent surface covering, making it excellent for long-term solar photovoltaic applications.[26,27] Following satisfactory coating, the slides were oven-dried for 3 h at 250°. The preparation of the dual functional coating followed a systematic chemical procedure involving all the mentioned chemicals.

The mechanism of the chemical reactions involved in the synthesis of HMDS-modified nano-silica surface coatings has been illustrated in Fig. 2. The figure shows that the diisopropylethylamine used in the preparation procedure acts as a strong base that detaches the H^+ from the hydroxyl group's silicate part, creating a strong nucleophilic species that the HMDS can readily attack. Finally, the activated nucleophilic species on the silica surface leads to the sophisticated attachment of the HMDS, producing the desired anti-reflective and anti-soiling properties of the synthesized coatings.

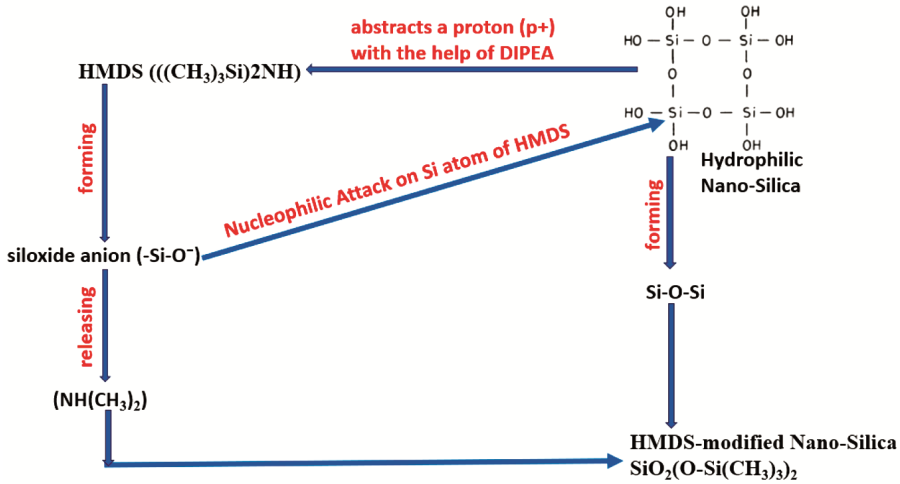

Fig. 2 — Schematic layout illustrating the molecular mechanism in creating the modified hydrophobic nano-silica coating

Characterization

A D/max 2200 PC diffractometer was used to observe X-ray diffraction (XRD). High-resolution Field Emission Scanning Electron Microscopy (FESEM) (ZEISS, 10 kV) was performed to depict the detailed characteristics of the surface morphology concerning the prepared coatings. The Water Contact Angles (WCA) were measured using the CA100A equipment, and a controlled 5 µL droplet size of deionized water was used for testing. Fourier Transform Infrared (FTIR) spectroscopy was used to identify the chemistry of the chemical compounds on the surface. Spectrum capture was performed in the 400–4000 cm^{-1} frequency band. The transmittance spectrum of the dual-functional coating was measured using a Cary 100 UV/vis spectrophotometer with a wavelength range of 200–800 nm. A variable angle spectral ellipsometer was used to measure the coating thickness and refractive index.

Experimental Setup

To investigate the environmental impact of dusty particulates on the operational effectiveness of solar photovoltaic cells, the operational efficiency of uncoated and coated cells was experimentally investigated under dusty conditions. The research was conducted at the Government Engineering College Jabalpur in the Applied Physics Laboratory (23.2012° N, 80.0012° E, Madhya Pradesh). The PV cells were erected on the laboratory's rooftop following the site's latitude to ensure maximum energy production during the testing period. Data measurements were collected for 77 days between April 1 and June 16, 2023. Two similar solar photovoltaic cells were utilized. The solar photovoltaic cell shown in Fig. 3(b) consisted of anti-reflective, anti-soiling, and super-hydrophobic nano-silica-HMDS coating with a 0.3:1 concentration ratio, regarded as the ideal concentration ratio. It was deemed to be a self-cleaning photovoltaic cell. The solar photovoltaic cell shown in Fig. 3(a) had no coating and was manually dusted and cleansed daily. Throughout each day for 77 days, the output power of the solar photovoltaic cells was measured and analyzed. The field study apparatus is represented in Fig. 3.

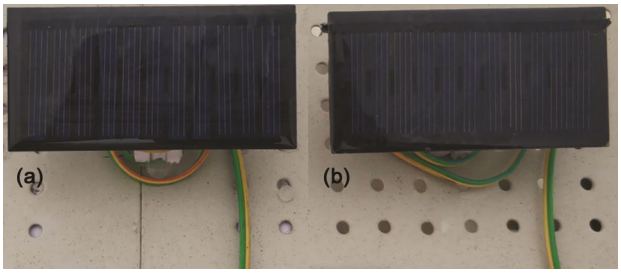

Fig. 3 — Image of the field study apparatus during measurement activity: (a) uncoated solar cell with manual cleaning, (b) self-cleaning solar cell coated with Nano-Silica & HMDS coating in (0.3:1)

Results and Discussion

XRD Study

Wave radiation in the 2θ range from 10° to 80° was used for testing the samples. The Braggs reflections measured by the X-ray diffraction spectra for HMDS base-catalyzed silica nanoparticles between the radiation intensity in angstrom units and 2θ angles in degrees (°) are depicted in Fig. 4 . A large peak is obtained at a 2θ angle of 23°, showing the presence of silica nanoparticles. The observed sharp peak at 23° in the XRD pattern of the produced nano-coating consisting of silica nanoparticles and HMDS illustrates that the silica involved is amorphous and represents silica (SiO_2). The amorphous structure ensures a uniform, isotropic surface, minimizing light scattering.[28] The substantially broader diffraction peaks suggest that the synthesized finely powdered particles were nanosized. The peaks show the purity of the silica nanoparticles. Bragg's reflections convincingly demonstrated the absence of lattice plane sets with the revelation of small crystallite sizes of the silica nanoparticles generated in our present synthesis, revealing their amorphous nature.[28]

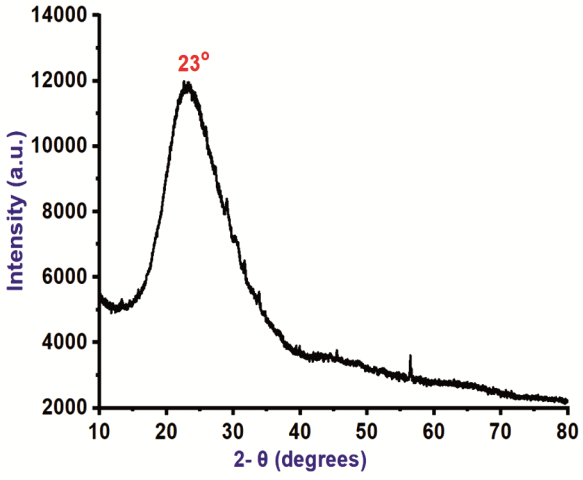

Fig. 4 — X-ray diffraction pattern of an anti-reflective coating consisting of Nano-Silica-HMDS

FTIR Study

Fourier Transform Infrared Spectroscopy (FTIR) was conducted to understand the chemical nature of thefabricated nano-coating. The FTIR spectrum of the produced surface coating is shown in Fig. 5. The spectrum was analyzed for a frequency range of 400 to 4000 cm^{-1}. As evident in the Nano-silica-HMDS FTIR spectrum is shown in Fig. 5, the broadband and a sharp peak near 3436 cm^{-1} can be observed. This corresponds to the remaining absorbed water and the O-H (hydroxyl) group stretching, owing to the partial condensation of the Si-OH (silanol) group.

The strength of the absorption peak diminishes as the quantity of HMDS involved with the modification increases, indicating that the O-H (hydroxyl) groups on the surface of the nano-silica are replaced by hydrophobic trimethyl silyl (-$Si(CH_3)_3$) groups leading to successful chemical modification of nano-silica by hexamethyldisilazane (HMDS).[29] Furthermore, Nano-silica-HMDS exhibits absorptance maxima around 1127 cm^{-1} representing Si-O-Si stretching vibrations, 1389 cm^{-1} representing O-H bond bending, 1631 cm^{-1} representing N-H Bending, an absorbance band from 2860 cm to 2931 cm^{-1} represents C-H bond stretching vibrations, andfinally, 3436 cm^{-1} represents O-H bond and N-H bond stretching vibrations. Additionally, an absorption band arises at 587 cm^{-1}, corresponding to the distinctive Si-C stretching vibrations observed in nano-silica samples modified by HMDS. Finally, the FTIR maxima correlated with the C-H (hydrocarbon) group stretching vibration, associated with HMDS, suggests that the HMDS has been chemically bonded to the nano-silica surface.

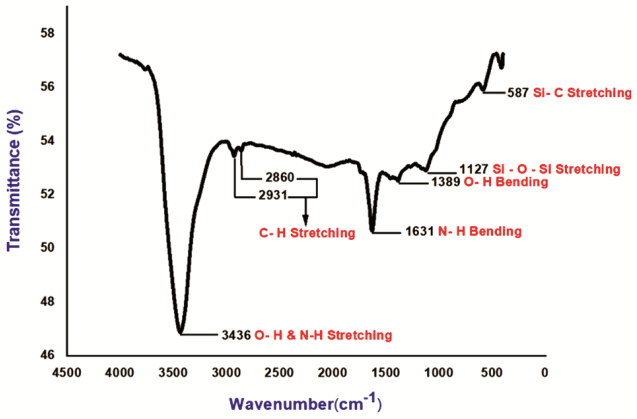

Fig. 5 — FTIR spectra of the prepared anti-reflection and anti-soiling coatings

WCA Study

The Cassie-Baxter and Wenzel models have been typically used to describe the hydrophobic attributes of high-roughness coatings. As a result, according to the Wenzel model, water droplets attach to a rough surface by following its profile, rendering movement over it impossible. Water droplets tended to glide across the surface of silica nanoparticle samples, showing that the Cassie-Baxter theory suitably justified the attained experimental data.[30] Hence, the experimental result for Water Contact Angle (WCA) analysis isrepresented by the following mathematical equation:

$$f_2 + f_1 = 1 \quad \ldots (1)$$

In the above mathematical equation, the proportion of air particles in contact with globules of water particles is defined by *f2,* and a portion of the solid surface in contact with globules of water particles is represented by *f1*.

Further, the mathematical representation of Cassie's equation can be shown as follows :

$$\theta_A = cos^{-1}(f_1 \cos\theta - f_2) \quad \ldots (2)$$

In the above equation, the notations *f1* and *f2* have the same meaning as mentioned below the Eq. (1), whereas the apparent contact angle recorded on the unmodified nano-silica substrate surface is represented by θ_A. The water contact angle on a smooth glass surface is represented by θ in Eq. (2), yielding a value of 29.5°. With the average water contact angle of 156° for constituent A shown in Table 1 (considered to be the best composition, which is nano-silica: HMDS in 0.3:1), the computed value of *f1* is 5.81%, indicating that the surface held by air is approximately 95%. This further indicates that the combination of silica nanoparticles with HMDS makes it easy for air to be entrapped, forming

Table 1 — shows WCA analysis concerning silica nanoparticles + HMDS and their varying transparency with different concentration ratios

Constituent	Nano-Silica-HMDS ratio	Water contact angle (degrees)	Nature of hydrophobicity	Nature of transparency
A	0.3:1	156	Super Hydrophobic	Excellent
B	0.5 :1	147	Hydrophobic	Very Good
C	1:1	134	Hydrophobic	Good
D	1:0.5	121	Hydrophobic	Satisfactory
E	1:0.3	110	Hydrophobic	Satisfactory

a surface with superhydrophobicity traits. The detailed information on the effect of varying the concentrations of the silica nanoparticles with that of the HMDS is provided in Table 1.

The water contact angle analysis of the varying concentrations of silica nanoparticles to the HMDS viz. 0.3:1, 0.5 :1, 1: 1, 1: 0.5, and 1: 0.3 concerning the original glass surface were performed and were respectively analyzed along with the nature of their hydrophobicity shown in Fig. 6.

The transparency of the varying silica nanoparticles with HMDS has been assessed demonstratively, as shown in Fig. 7. In general, transparency and superhydrophobicity are mutually contradictory because an increase in superhydrophobicity resulting from the surface roughness might result in reduced transparency. An increase in silica concentration above a specific limit can result in increased hydrophobicity but reduced transparency.[31] Hence, the appropriate concentration of nano-silica is one of the most significant and crucial variables in fabricating transparent superhydrophobic coatings.

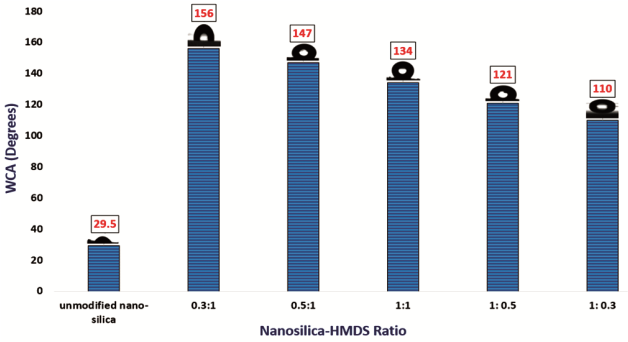

Fig. 6 — WCA analysis of the prepared anti-reflection and anti-soiling coatings

Considering the above observations, the test results represent the Nano-Silica-HMDS, with (0.3:1) being the optimum concentration for achieving hydrophobicity, anti-soiling, and anti-reflection properties simultaneously.

Optical Transmission Studies

The average transmissivities of uncoated glass, Nano-Silica coating, and Nano-Silica-HMDS coating are shown in the optical transmittance spectra (Fig. 8(a)), with values of 93.2%, 95.2%, and 96.1%, respectively. Because superhydrophilic SiO_2 and airborne water molecules are adsorbed on nano-silica-HMDS, its average transmissivity was superior to that of nano-silica coating. The superhydrophilic surface became superhydrophobic upon the introduction of $-CH_3$, and the refractive index was lowered by air rather than water. Due to the additional reflection of incoming light, the mean transmittance of nano-silica-HMDS rose by around 3.1% when compared to that of uncoated glass and

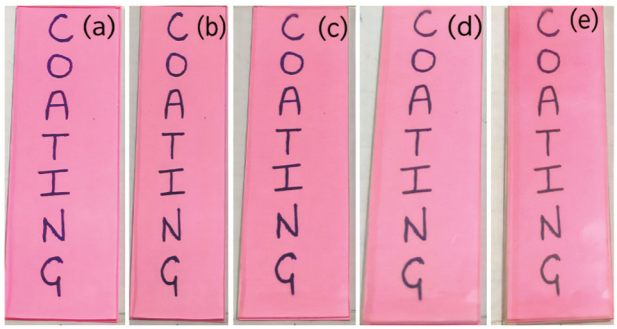

Fig. 7 — Transparency effects with the variation of silica concentration along with HMDS for the following nano-silica- HMDS coatings in ratios: (a) 0.3:1; (b) 0.5:1; (c) 1:1; (d) 1:0.5; and (e) 1:0.3

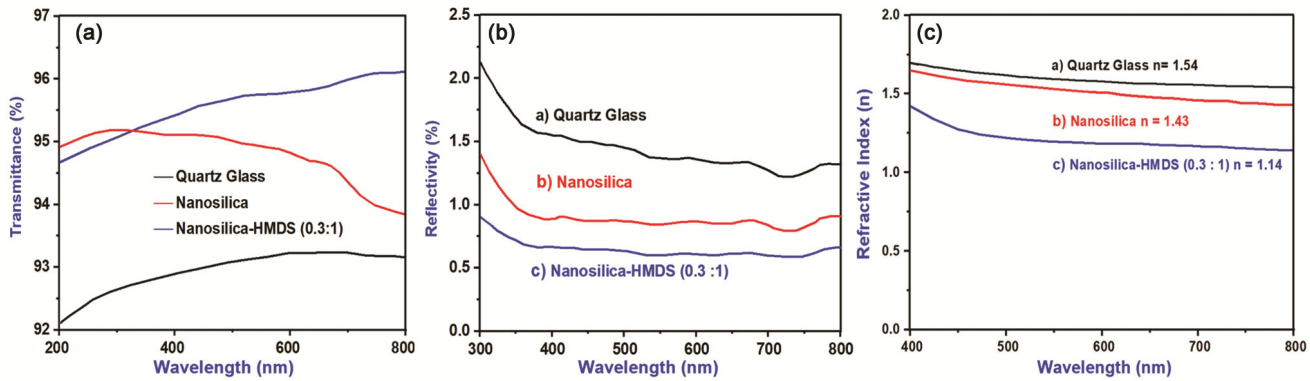

Fig. 8 — Comparison of Uncoated Glass, Nano-Silica coating, and Nano-Silica-HMDS coating: (a) Transmittance spectra, (b) Reflectivity Spectra (c) Refractive index

around 1.1% when compared to nano-silica alone. The diffuse reflectivity curves of uncoated glass, nano-silica coating, and nano-Silica-HMDS coating (Fig. 8(b)) showed that the coating had an anti-reflection property and that the nano-Silica-HMDS coating possessed a lower reflection index as compared to the nano-silica coating and uncoated glass (Fig. 8(c)). Both the optical spectra (transmittance and refractive index) and reflectance spectra produced consistent results.

Surface Morphology Study

The nano-structural and morphological characteristics of the fabricated anti-reflective and anti-soiling coatings are shown in Fig. 9. Studies have shown that anti-reflection and anti-soiling coatings have a permeable and transparent form resulting from nano-silica assemblage. The generated surfaces (as evident from the FESEM images of Fig. 9a and 9b) are the result of an alkali-catalyzed hydrolysis and condensation process, which produces nano-nuclei. The reactive agents proceed to gather and develop on the reacting surface's external layers, forming nano-sized particles progressively.[32–34] The surface produced is homogeneous because the hexamethyldisilazane reacts alongside the O-H group on the nano-silica surface to fill the voids, so the prepared nano-coating has an improved surface finish and optimal transmittance (Fig. 9b).

In addition, introducing di-isopropyl ethyl amine is beneficial to transparency, and introducing hexamethyldisilazane is beneficial to hydrophobic properties. The nano-silica and nano-silica-HMDS coatings FESEM results (represented in Fig. 9(a) and 9(b)) revealed that they were made of aggregated nanoparticles ranging in size from 30 to 50 nm and were widely distributed with many nanopores within. The size of the particles remained unchanged after the addition of HMDS suggesting that the hexamethyldisilazane primarily interacted with the particle surfaces without affecting their overall structural integrity. The root mean square roughness of the nano-silica and the nano-silica-HMDS coatings as obtained from the images of the AFM analysis, (as shown in Fig. 9(c) and 9(d)) was 4.38 nm and 10.89 nm respectively. High transmittance was anticipated despite the coated surface being roughened with HMDS treatment since the root mean square roughness value obtained was less than 100 nm.

HMDS accumulates in external layers on the anti-reflective nano-coating surface to pack the voids while reducing the coating's surface coarseness, which is compatible with the preceding rationale. Hence, an effective anti-reflective and superhydrophobic coating can be fabricated by filling the permeable matrix with the grafted hexamethyldisilazane and adding di-iso propyl ethyl amine.

Assessment of the Stability of Coatings

Erosion due to weather effects gradually depletes the surface of the coatings, reducing their life. Hence, assessment of the life of the coatings is essential. The

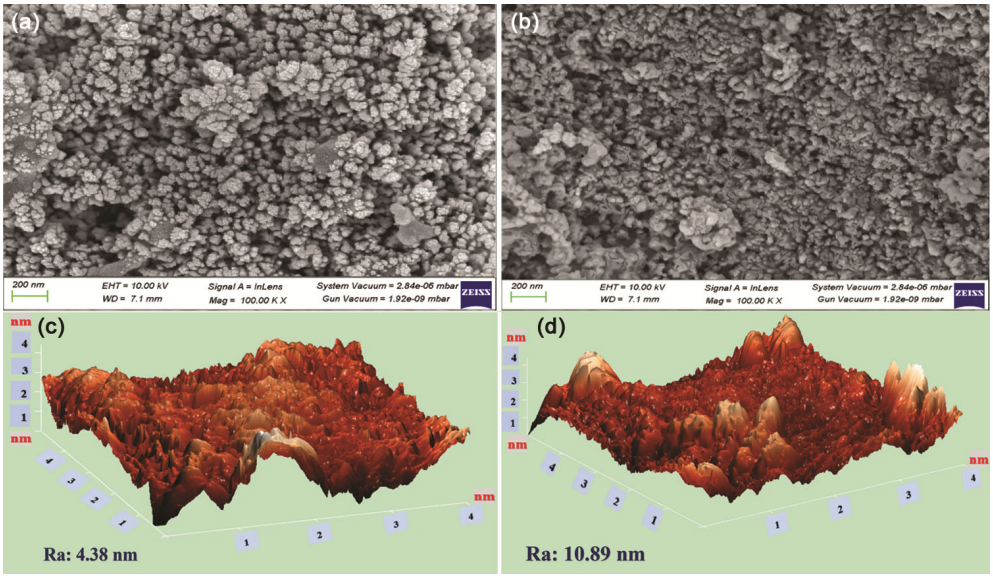

Fig. 9 — FESEM image of (a) Nano-silica coating and (b) Nano-silica-HMDS coating, (c) AFM Image of Nano-silica coating and (d) Nano-silica-HMDS coating

stability of the coatings is an essential characteristic as it ensures an enduring and cost-efficient coating.

Furthermore, good stability eliminates the requirement for frequent coating application. The coating with a Nano-Silica & HMDS ratio of 0.3 :1 was selected to assess weather erosion and stability because of its excellent superhydrophobicity and transparency attributes compared with other ratios. The coating was tested in an open environment for 2.5 months from April to mid-June 2023, and the coated surface was found to be stable for approximately two months.

The anti-reflection and anti-soiling effect of the superhydrophobic nanomaterial coating were demonstrated by measuring the output power of the two solar cells during the day. By permitting typical atmospheric dust to accumulate on the top layer of solar cells, the anti-reflection and anti-soiling impact of the nano-silica-HMDS coating were examined.

The prevalent particulate matter (including dust particles) size analysis data observed in the region of the experimental setup taken from the Madhya Pradesh Pollution Control Board (Jabalpur Air Quality Index platform) is shown in Table 2. An experimental setup of uncoated and coated solar cells was tested in an open environment to test the anti-soiling effect when exposed naturally to the prevalent samples of dust particles of different sizes, as mentioned in Table 2. The average distribution of the prevalent pm 2.5 and pm 10 in the local atmosphere of the experimental setup is shown in Fig. 10 (a) and 10 (b).

The average particle size based on the anti-soiling principle is ~10 µm shown in Fig. 11. The addition of hexamethyldisilazane causes the nano-silica to make less contact with the particle surface, resulting in a

Table 2 — Particle size analysis of particulate matter (including dust) at the experimental site

S no.	Sample	Average Size (µm)
1	PM 2.5	1–2.5
2	PM 10	2.5–10

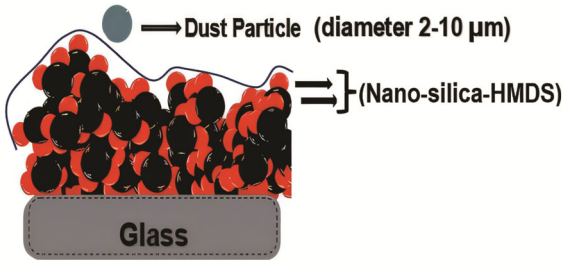

Fig. 11 — Anti-soiling phenomenon of the prepared coating

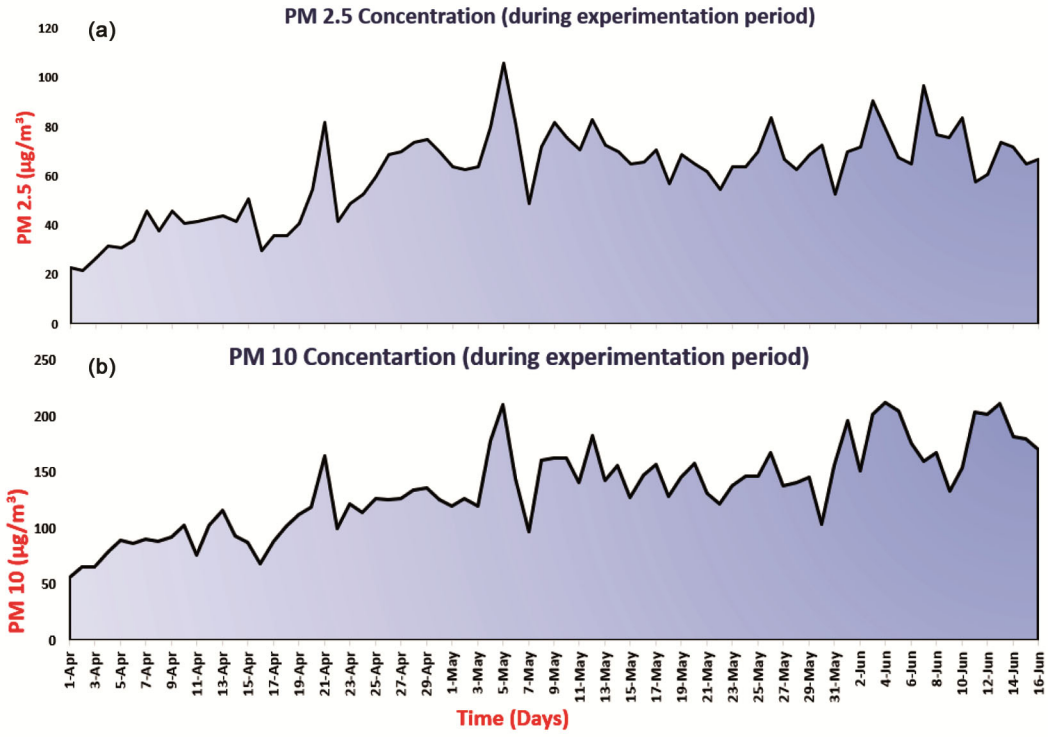

Fig. 10 — Images of the dominant: (a) pm 2.5 and (b) pm 10, in the local atmosphere of the experimental setup during the testing period; The -axis shows particulate matter concentrations in µg/m3 and the X-axis shows the time in days

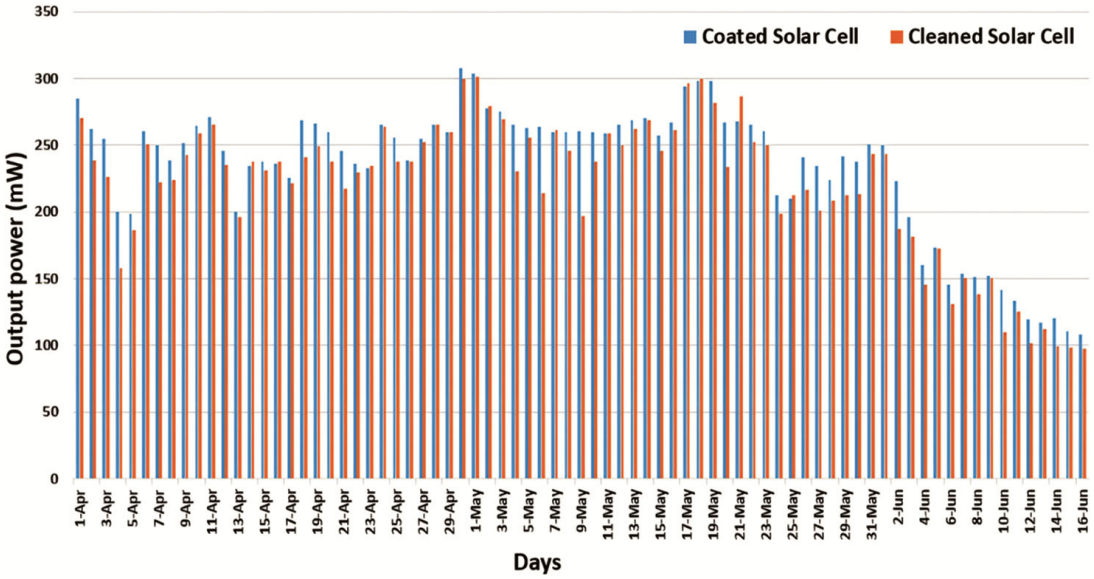

Fig.12 — The average power produced by the two solar cells; A coated solar cell is a self-cleaning solar cell with an HMDS-modified nano-silica surface coating, A cleaned Solar cell is a manually cleaned solar cell with no surface coating

fractal structure. Also, the charged particles escape the antistatic dust and do not gather on the surface.[35,36] Furthermore, in an open environment, the enhanced output power related to the coated solar photovoltaic cell compared to the uncoated solar photovoltaic cell exposed to particulate matter, including dust particles, proves that the coating successfully achieved the anti-soiling characteristics.

The output power of the two solar cells considering the regional atmospheric temperature and sun irradiance was measured every day for 77 days. Finally, the daily mean values were determined.

According to the results of this experiment, the application of nano-silica-HMDS superhydrophobic anti-reflective coating would boost the output power and overall efficiency of the photovoltaic cells (as depicted and shown in Fig. 12). This is the consequence of the capacity of the solar cell's coating to clear dust with no additional effort. The nano-silica-HMDS nanomaterial coating's antistatic effect leads to the spreading away of the globules of water, resulting in a minute film with low photon obstruction. The small water droplets combine and readily flow down the panel's surface (Fig. 3 and Fig. 6). The progression of water droplets on the top surface will cause dust particles to descend, as opposed to the uncoated solar cell, which might generate a coating of muck on the cell's top surface.[37,38] Hence, upon nano-coating of the surface, the self-cleaning process improves, increasing the total efficiency of the nano-silica-HMDS-coated solar photovoltaic cell. The study also discovered that the anti-reflection effect of nano-silica-HMDS nanocoating improves the overall output power performance of the solar cell (Fig. 9 and Fig. 12), by additionally having the ability to reduce the temperature of the solar cell due to less resistance offered to photons[35,36], which is approximately 5.8% higher in comparison to the physically cleansed uncoated solar cell at peak sun radiation each day.

Conclusions

In summary, dual-functional nano-silica-HMDS coatings with anti-reflective and anti-soiling properties were developed using an efficient and cost-effective dip-coating method. The XRD and FTIR tests validate the amorphous nature and successful nano-silica surface modification by HMDS. The optimal coating nano-silica to HMDS in 0.3:1 reached a WCA of 156°, exhibiting superhydrophobicity. It demonstrated excellent surface finish and optical clarity owing to HMDS reaction with O-H groups on nano-silica, filling tiny voids confirmed by transparency tests and AFM roughness measurements below 100 nm. It showed a remarkable transmissivity of 96.1%, improving 3.1% compared to uncoated glass and 1.1% to nano-silica. The optimal coating remained stable over 2.5 months in dusty and regional atmospheric conditions, improving coated solar cell efficiency by 5.8% compared to uncoated cells. These

coatings suit solar panels, optical screens, windows, and architectural glass, particularly in dusty and tropical environments. Future studies could use machine learning models to predict coating durability, enabling faster optimization and reducing long-term testing requirements.

Acknowledgment

The authors hereby acknowledge IIT Ropar, IIT Roorkee, and CRS laboratory, Applied Physics, JEC, Jabalpur, M.P., India for using synthesis and characterization facilities.

References

1 Keshavarzi R, Molabahrami N, Afzali N & Omrani M, Improving efficiency and stability of carbon-based perovskite solar cells by a multifunctional triple-layer system: Antireflective, uv-Protective, superhydrophobic, and self-cleaning, *Solar RRL*, **4** (2020) 2000491, https://doi.org/10.1002/solr.202000491.

2 Sun X, Tu J, Li L, Zhang W & Hu K, Preparation of wide-angle and abrasion-resistant multi-layer antireflective coatings by MgF2 and SiO2 mixed sol, *Coll Surf A*, **602** (2020) 125106, https://doi.org/10.1016/j.colsurfa.2020.125106.

3 Zou X, Tao C, Yan L, Yang F, Lv H, Yan H, Wang Z, Li Y, Wang J, Yuan X & Zhang L, One-stepsol-gel preparation of ultralow-refractive-index porous coatings with mulberry-like hollow silica nanostructures, *Surf Coat Tech*, **341** (2018) 57–63, https://doi.org/10.1016/j.surfcoat.2018.01.013.

4 Xu L, Geng Z, He J & Zhou G, Mechanically robust, thermally stable, broadband antireflective, and superhydrophobic thin films on glass substrates, *ACS Appl Mater Interfaces*, **6(12)** (2014) 9029–9035, https://doi.org/10.1021/am5016777.

5 Zhang C & Xu Y, Transparent and hydrophobic hexylene-bridged polymethyl siloxane/sio2 composite coating with tunable refractive index and its application for broadband antireflection, *Thin Solid Films*, **701** (2020) 137944, https://doi.org/10.1016/j.tsf.2020.137944.

6 Xia B, Yan L, Li Y, Zhang S, He M, Li H, Yan H & Jiang B, Preparation of silica coatings with continuously adjustable refractive indices and wettability properties via sol-gel method, *RSC Adv*, **8** (2018) 6091–6098, https://doi.org/10.1039/C7RA12817G.

7 Tao C, Zou X, Reddy K M, Zhang L & Jiang B, A hydrophobic ultralow refractive-index silica coating towards double-layer broadband antireflective coating with exceptionally high vacuum stability and laser-induced damage threshold, *Coll Surf A*, **563** (2019) 340–349, https://doi.org/10.1016/j.colsurfa.2018.11.038.

8 Zhang L, Xue C H, Cao M, Zhang M M, Li M & Ma J Z, Highly transparent fluorine-free superhydrophobic silica nanotube coatings, *Chemical Eng J*, **320** (2017) 244–252, https://doi.org/10.1016/j.cej.2017.03.048.

9 Kong J H, Kim T H, Kim J H, Park J K, Lee D W, Kim S H & Kim J M, Highly flexible, transparent and self-cleanable superhydrophobic films prepared by a facile and scalable nanopyramid formation technique, *Nanoscale*, **6** (2014) 1453–1461, https://doi.org/10.1039/C3NR04629J.

10 Sethi S K & Manik G, Recent progress in super hydrophobic/hydrophilic self-cleaning surfaces for various industrial applications: A review, *Polym Plast Technol Eng*, **57** (2018) 1932–1952, https://doi.org/10.1080/03602559.2018.1447128.

11 Tavakoli M M, Tsui K H, Zhang Q, He J, Yao Y, Li D & Fan Z, Highly efficient flexible perovskite solar cells with antireflection and self-cleaning nanostructures, *ACS Nano*, **9** (2015) 10287–10295, https://doi.org/10.1021/acsnano.5b04284.

12 Lian Z, Xu J, Wang Z, Yu Z, Weng Z & Yu H, Nanosecond laser-induced underwater superoleophobic and underoil superhydrophobic mesh for oil/water separation, *Langmuir*, **34** (2018) 2981–2988, https://doi.org/10.1021/acs.langmuir.7b03986.

13 Ni X X, Jiang G C & Yang L L, The Synthesis of super-hydrophobic nano-silica and its effect on the surface wettability of sandstone, *Mater Sci Forum*, **917** (2018) 140–144, https://doi.org/10.4028/www.scientific.net/MSF.917.140.

14 Dong S, Zhang X, Li Q, Liu C, Ye T, Liu J, Xu H, Zhang X, Liu J, Jiang C, Xue L, Yang S & XiaoX, Springtail-inspired superamphiphobic ordered nanohoodoo arrays with quasi-doubly reentrant structures, *Small*, **16** (2020) 2000779, https://doi.org/10.1002/smll.202000779.

15 Richards B S, Comparison of TiO2 and other dielectric coatings for buried-contact solar cells: A review, *Progress Photovoltaics*, **12(4)** (2004) 253–281, https://doi.org/10.1002/pip.529.

16 Pern F J, Panosyan Z H, Gippius A A, Kontsevoy J A, Touryan K, Voskanyan S & Yengibaryan Y, Diamond-like carbon coatings as encapsulants for photovoltaic solar cells, *Conference Record of the Thirty first IEEE Photovoltaic Specialists Conference* (Lake Buena Vista, FL, USA) 2005, 1339–1342.

17 Rao A V, Latthe S S, Nadargi D Y, Hirashima H B & Ganesan V, Preparation of MTMS based transparent superhydrophobic silica films by sol-gel method, *J Colloid Interface Sci*, **332(2)** (2009) 484–490, https://doi.org/10.1016/j.jcis.2009.01.012.

18 Zhi J & Zhang L Z, Durable superhydrophobic surface with highly antireflective and self-cleaning properties for the glass covers of solar cells, *Appl Surf Sci*, **454** (2018) 239–248, https://doi.org/10.1016/j.apsusc.2018.05.139.

19 Yin X, Yu S, Bi X, Liu E & Zhao Y, Robust superhydrophobic 1D Ni3S2 nanorods coating for self-cleaning and anti-scaling, *Ceram Int*, **45(18)** (2019) 24618–24624, https://doi.org/10.1016/j.ceramint.2019.08.192.

20 Jang G G, Smith D B, Polizos G, Collins L, Keum J K & Lee D F, Transparent superhydrophilic and superhydrophobic nanoparticle textured coatings: A comparative study of anti-soiling performance, *Nanoscale Adv*, **1(3)** (2019) 1249–1260, https://doi.org/10.1039/c8na00349a.

21 Liu E, Yin X, Hu J, Yu S, Zhao Y & Xiong W, Fabrication of a biomimetic hierarchical superhydrophobic Cu-Ni coating with self-cleaning and anti-corrosion properties, *Coll Surf A*, **586** (2020) 124223, https://doi.org/10.1016/j.colsurfa.2019.124223.

22 Zhao X & Murphy M C, A High-adhesion binding strategy for silica nanoparticle-based superhydrophobic coatings, *Coll*

Surf A: Physicochem Eng Aspects, **625** (2021) 126810, https://doi.org/10.1016/j.colsurfa.2021.126810.

23 Ge Q & Liu H, Rational design, and preparation of superhydrophobic photo-cured hybrid epoxy coating modified by fluorocarbon substituted silsesquioxane-based nanoparticles, *Prog Org Coat*, **172** (2022) 107089, https://doi.org/10.1016/j.porgcoat.2022.107089.

24 Li W & Liu H, Design, and preparation of SQ-based superhydrophobic coatings with different substituents for multifunctional applications, *Surf Coat Technol*, **457** (2023) 129285, https://doi.org/10.1016/j.surfcoat.2023.129285.

25 Wang P, Zeng J, Yan X, Tan P, Wang M, Zheng Y, Shen Y, Chen J, Nie Y & Liu S, A three-layer superhydrophobic coatings inspired by human scalp structure with excellent anti-reflection and durable effects for photovoltaic applications, *J Clean Prod*, **414** (2023) 137605, https://doi.org/10.1016/j.jclepro.2023.137605.

26 Butt M A, Thin-Film coating methods: A successful marriage of high-quality and cost-effectiveness- A brief exploration, *Coatings*, **12(8)** (2022) 1115, https://doi.org/10.3390/coatings12081115.

27 Sriram S, Singh R K & Kumar A, Silica and silane based polymer composite coating on glass slide by dip-coating Method, *Surf Interfaces*, **19** (2020) 100472, https://doi.org/10.1016/j.surfin.2020.100472.

28 Zhang Q, Liu H, Zhao S & Dong W, Hydrophobic and optical properties of silica antireflective coating prepared via sol-gel method, *Mater Res Express*, **8** (2021) 046403, http://doi.org/10.1088/2053-1591/abf6fb.

29 Bingbing X & Qiuhui Z, Preparation and properties of hydrophobically modified nano- SiO2 with hexadecyltrimethoxysilane, *ACS Omega*, **6(14)** (2021) 9764–9770, https://doi.org/10.1021/acsomega.1c00381.

30 Liu J, Janjua Z A, Roe M, Xu F, Turnbull B, Choi K S & Hou X, Super-hydrophobic/icephobic coatings based on silica nanoparticles modified by self-assembled monolayers, *Nanomaterials*, **6(12)** (2016) 232, https://doi.org/10.3390/nano6120232.

31 Yu S, Guo Z & Liu W, Biomimetic transparent and superhydrophobic coatings: from nature and beyond nature, *Chem Commun*, **51(10)** (2015) 1775–1794, https://doi.org/10.1039/C4CC06868H.

32 Zhao X, Wang Y, Luo J, Wang P, Xiao P & Jiang B, The influence of water content on the growth of the hybrid-silica particles by sol-gel method, *Silicon*, **13** (2021) 3413–3421, https://doi.org/10.1007/s12633-020-00756-z.

33 Yoldas B E & Partlow D P, Formation of broad band antireflective coatings on fused silica for high power laser applications, *Thin Solid Films*, **129(1)** (1985) 1–14, https://doi.org/10.1016/0040- 6090(85)90089-6.

34 Guo Z Q, Liu Y, Tang M Y, Wang J H & Su X P, Super-durable closed-surface antireflection thin film by silica nanocomposites, *Solar Energ Mat Solar Cells*, **170** (2017) 143–148, https://doi.org/10.1016/j.solmat.2017.05.043.

35 Oh W, Kang B, Choi S, Bae S, Jeong S, Kim S M, Lee H S, Kim D, Hwang H & Chan S, Evaluation of anti-Soiling and anti-reflection coating for photovoltaic modules, *J Nanosci Nanotechnol*, **16** (2016) 10689–10692, https://doi.org/10.1166/jnn.2016.13219.

36 Che Y, Synthesis, characterization, and application of silica aerogel thin films prepared via surface derivatization: A comprehensive study on micro-silica nanofilms for enhanced photoelectric conversion efficiency in photovoltaic solar cells, *Proc 4th Int Conf Mater Chem Environ Eng* (The Loomis Chaffee School, Windsor, CT 06095, USA) 2024, 99–119.

37 Samadhiya A, Jhinge P K & Kushwah K K, Experimental investigation on synthesis and characterization of self-cleaning modified super hydrophobic nano-Sio_2 coating for solar photovoltaic applications: Effects of HDTMS and TEA, *Indian J Eng Mater Sci*, **30** (2023) 588–596, https://doi.org/10.56042/ijems.v30i4.386.

38 Ahmed A, Elsakka M, Elhenawy Y, Amer A, Mansi A, Bassyouni M, Gadalla M & Refaat A, Experimental investigation of a nano coating efficiency for dust mitigation on photovoltaic panels in harsh climatic conditions, *Sci Rep*, **14** (2024) 23013, https://doi.org/10.1038/s41598-024-72772-7.